International Journal of Nanomedicine

Dovepress
open access to scientific and medical research

Open Access Full Text Article

ORIGINAL RESEARCH

Combined ROS Sensitive PEG-PPS-PEG with Peptide Agonist for Effective Target Therapy in Mouse Model

Pingping Xiang[1,2,*], Qi Liu[1,3,*], Wangwei Jing[1,4], Yaping Wang[1], Hong Yu[1,5,6]

[1]Department of Cardiology, The Second Affiliated Hospital, Zhejiang University School of Medicine, Hangzhou, Zhejiang Province, 310009, People's Republic of China; [2]Key Laboratory of Multiple Organ Failure (Zhejiang University), Ministry of Education, Hangzhou, Zhejiang Province, People's Republic of China; [3]Department of Cardiology, Sir Run Run Shaw Hospital, Zhejiang University School of Medicine, Hangzhou, Zhejiang, People's Republic of China; [4]Department of Cardiology, Affiliated Hangzhou First People's Hospital, School of Medicine, Westlake University, Hangzhou, Zhejiang, People's Republic of China; [5]State Key Laboratory of Transvascular Implantation Devices, Hangzhou, 310009, People's Republic of China; [6]Binjiang Institute of Zhejiang University, Hangzhou, 310053, People's Republic of China

*These authors contributed equally to this work

Correspondence: Hong Yu; Yaping Wang, Tel +86-571-87783992, Fax +86-571-88002709, Email yuvascular@zju.edu.cn; yapingwang@zju.edu.cn

Background and Purpose: Growth hormone-releasing hormone (GHRH) agonist, a 29-amino acid peptide, shows significant potential in treating myocardial infarction (MI) by aiding the repair of injured heart tissue. The challenge lies in the effective on-site delivery of GHRH agonist. This study explores the use of a targetable delivery system employing ROS-responsive PEG-PPS-PEG polymers to encapsulate and deliver GHRH agonist MR409 for enhanced therapeutic efficacy.

Methods: We synthesized a self-assembling poly (ethylene glycol)-poly (propylene sulfide)-poly (ethylene glycol) polymer (PEG-PPS-PEG) amphiphilic polymer responsive to reactive oxygen species (ROS). The hydrophilic peptide GHRH agonist MR409 was encapsulated within these polymers to form nano PEG-PPS-PEG@MR409 vesicles (NPs). Cardiomyocyte apoptosis was induced under hypoxia and serum-free culture condition for 24 hours, and their production of ROS was detected by fluorescence dye staining. The cellular uptake of PEG-PPS-PEG@MR409 NPs was observed using fluorescence-labeled MR409. Targeting ability and therapeutic efficacy were evaluated using a mouse MI model.

Results: PEG-PPS-PEG@MR409 NPs were efficiently internalized by cardiomyocytes, reducing ROS levels and apoptosis. These NPs exhibited superior targeting to the infarcted heart compared to naked MR409 peptide. With a reduced injection frequency (once every three days), PEG-PPS-PEG@MR409 NPs significantly promoted cardiac function recovery post-MI, matching the efficacy of daily MR409 injections.

Conclusion: ROS-responsive PEG-PPS-PEG polymers provide a novel and effective platform for the targeted delivery of GHRH agonist peptides, improving cardiac function and offering a new approach for peptide therapy in MI treatment.

Keywords: myocardial infarction, targeted therapy, growth hormone-releasing hormone, reactive oxygen species

Introduction

Myocardial infarction (MI) poses a major threat to human health and life due to its high morbidity and mortality.[1] Growth hormone-releasing hormone (GHRH) agonists have been demonstrated to prevent cardiomyocyte apoptosis[2,3] and ameliorate myocardial injury after acute infarction by activating reperfusion injury repair kinase (RISK) and survival activator enhancement (SAFE) pathways.[4] GHRH-agonist peptides may be a new promising therapeutic agent to prevent apoptosis of CMs and reduce fibrosis after MI independently of growth hormone (GH) or insulin-like growth factor I (IGF-I).[5] They have several advantages as peptides over proteins or antibodies: easy to synthesize, high specificity and low toxicity. Despite their potential, GHRH agonists face challenges such as instability and a short half-life.[6] Additionally, GHRH receptors are expressed in various tissues, which may lead to potential off-target effects.[7–9] Thus, there is an urgent need to develop strategies to enhance the targeted release and stability of GHRH agonists.

Received: 30 May 2024
Accepted: 13 August 2024
Published: 5 September 2024

Graphical Abstract

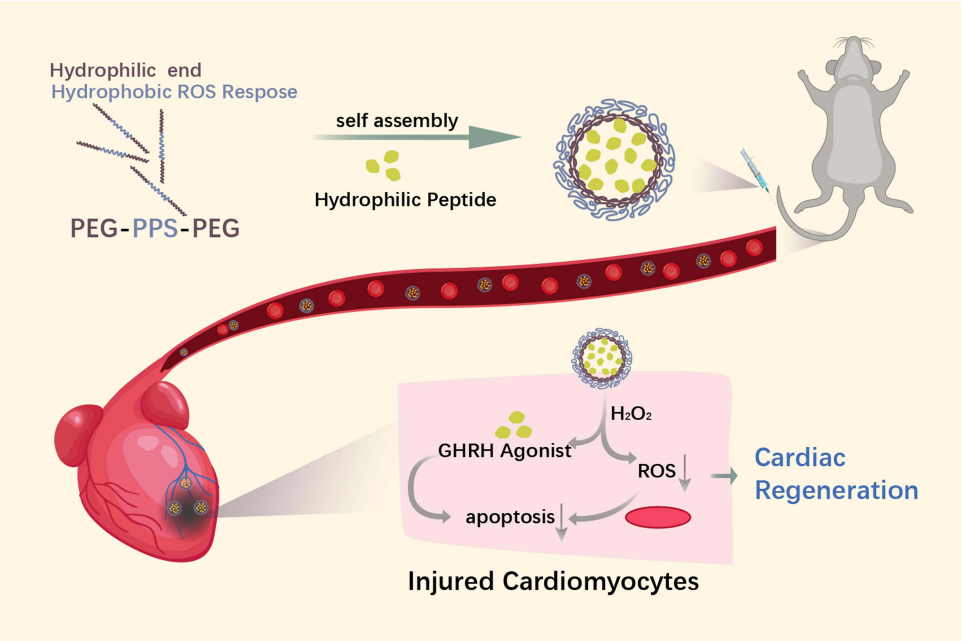

The application of nanotechnology in medicine is at the forefront of modern medicine and health care because it represents an effective treatment method.[10–12] In recent years, a series of first-generation nanoproducts have been approved for clinical use, and liposome and polymer drug conjugated nano-systems are also under clinical and preclinical development.[13–15] Recently, the drug delivery systems (DDSs) have attracted more and more attentions because DDSs are able to effectively deliver many kinds of therapeutic drugs to the target tissues/organs.[16] One of the most popular biological stimuli is the reactive oxygen species (ROS) for the disease development. ROS-responsive DDSs have shown great potential in a series of biomedical applications, such as targeted therapy for cancer or inflammation related diseases.[17,18] In the ischemic myocardium, ROS are massively generated. Additionally, it has been demonstrated that ROS-responsive fluorescent nanoparticles were highly specific targeted to the ischemic/perfused myocardium through the first 24h post reperfusion.[19]

Herein, we propose an alternative design of NPs featuring ROS-responsive release of drug for on-site therapy. The NPs were fabricated by self-assembly of ROS responsive poly (ethylene glycol)-poly (propylene sulfide)-poly (ethylene glycol) polymer (PEG-PPS-PEG) amphiphilic polymers. Hydrophilic peptides, GHRH agonist MR409, were loaded in the inner core of the vesicles (denoted as PEG-PPS-PEG@MR409 NPs). The protective characteristics of the NPs include improved bioavailability, reduced biodegradation, and increased selectivity to the injured heart after MI. We found that PEG-PPS-PEG@MR409 NPs had an efficient therapeutic effect on MI, and reduced the number of treatments to reach similar protective effect as the direct injection of peptide.

Materials and Methods

Preparation of Poly (Ethylene Glycol)-Poly (Propylene Sulfide)-Poly (Ethylene Glycol) Polymer

Synthesis of PEG-Tosyl

A 1.5-g poly (ethylene glycol) methyl ether (Sigma-Aldrich, Mw ~ 1 kDa) was dissolved in 20 mL of a 1:1 (v:v) tetrahydrofuran (THF)/water mixture, then 4.0 g sodium hydroxide was added over an ice bath with vigorous stirring. Excess tosyl chloride (5.0 g) dissolved in 15 mL THF was added drop-wise to the above solution. After overnight reaction

under ambient conditions, the solution was extracted three times with dichloromethane and distilled water. The transparent viscous liquid PEG-Tosyl was obtained by removing the solvent.

Synthesis of PEG Thioacetate

A 0.9-g sample of PEG-Tosyl was dissolved in 20 mL of dichloromethane and 2.28 g potassium thioacetate dissolved in 20 mL of a 1:1 dichloromethane/MeOH mixture was added. Following addition of 500 μL trimethylamine, the mixture was incubated for 12 h. The precipitate was filtered and the solvent was removed using a rotavapor. The remaining product was extracted three times with dichloromethane and distilled water. The transparent viscous liquid PEG thioacetate was obtained by removing the solvent.

Synthesis of PEG-PPS-PEG Triblock Polymer

A 200-mg sample of PEG thioacetate was dissolved in 5 mL THF and the solution degassed three times with nitrogen. A 16-mg sample of sodium methoxide in 0.5 mL MeOH was injected into the degassed solution and the mixture left at room temperature for 30 min. Then, 925 mg propylene sulfide was injected into the mixture. After 45 min, 138 mg iodoacetamide was added and the new solution left overnight. The final product was obtained by precipitation with three volumes of ethyl ether.

Preparation and Characterization of MR409-Loaded Vesicles

MR409 was then loaded into PEG-PPS-PEG-based vesicles via a solvent exchange method. Briefly, amphiphilic PEG-PPS-PEG (5 mg) block copolymer was dissolved in 1 mL THF, followed by slow drop-wise addition to 2 mL of 0.1 μg/μL MR409 aqueous solution. The organic solvent was removed using a rotavapor and MR409-loaded vesicles were purified by three centrifugations at 4000×g (10 min/each) using an Amicon Ultra-15 centrifugal filter unit (Merck-Millipore, USA). Transmission electron microscopy (TEM) (HT7700, Hitachi, Japan) was used to examine vesicle morphology, and hydrodynamic diameter of vesicles was measured with dynamic light scattering (DLS, Zetasizer 3000, Malvern, Southborough, MA) at room temperature.

Fluorescent labeled MR409 was that [20] lysine was conjugated with fluorescein isothiocyanate (FITC) or near-infrared fluorescent probe Cy5 (Sangon, Shanghai, China), which was used to quantify vehicle loading and release of MR409. After PEG-PPS-PEG@MR409 NPs preparation and purification, the supernatant was collected and UV absorption measured to calculate the amount of MR409 analog released according to a standard curve. The vesicle/MR409 aqueous suspension was then stored at −20 °C until use.

Intracellular Reactive Oxygen Species (ROS) Assay

H9C2 rat myocardial cells were purchased from American Type Culture Collection(ATCC). Cell suspension of H9C2 cells or primary neonatal rat cardiomyocytes (NRCM) at concentration of 1×105 cells/mL was seeded 2 mL per well in six-well plates. H9C2 cells and primary neonatal rat cardiomyocytes (NRCM) were then divided into four groups. After hypoxia and serum-free condition for 24 hours, a 500 μL dichloro-dihydrofluorescein diacetate (DCFH-A) (Beyotime Biotechnology, Shanghai, China) diluted with serum-free medium was added and stained for 20–30 min. After washing with serum-free medium for three times, the cells were detected by flow cytometry (BD Biosciences, San Jose, CA, USA).

Annexin V/PI Staining to Detect Apoptosis

After washing with PBS, the harvested cells were incubated with Annexin V-FITC for 30 min according to the manufacturer's instruction (Dojindo, Minato-ku, Tokyo, Japan). After treatment, the cells were detected by flow cytometry (BD Biosciences, San Jose, CA, USA).

Ex vivo Imaging

Mice were subcutaneously injected with the Cy5 labeled PEG-PPS-PEG@MR409 NPs or the control solution, and sacrificed in 30 min later. The organs were collected for ex vivo imaging. Fluorescence images were obtained with IVIS

Lumina III imaging system (Perkin Elmer). Use the following acquisition parameters: excitation filter range: 680 to 740 nm, emission filter: 790 nm, exposure time: 2 seconds, grading factor 4, f/Stop: 2. Use Living Image 4.3.1 software (Perkin Elmer) for spectral decomposition, image processing and analysis.

Establishment of a Mouse Myocardial Infarction Model

All animal experiments were performed with approval of the Animal Use and Care Committee of Zhejiang University, which complies with the Guide for the Care and Use of Laboratory Animals, 8th edition published by the USA National Institutes of Health. The approval for the study was granted by the Ethics Review Committee from the Second Affiliated Hospital of Zhejiang University. Mice (C57BL/6) were anesthetized with isoflurane. All mice had free access to a normal diet and water. The mice were shaved and the skin was disinfected with 75% ethanol prior to operation. Male C57BL/6J mice (8–10 weeks, 22–25 g) were divided into four groups, each with 7–9 mice, namely PBS, MR409, PEG-PPS-PEG and PEG-PPS-PEG@MR409 NPs groups. Acute myocardial infarction was achieved by ligating the left anterior descending coronary artery.[21] Mice were anesthetized by subcutaneously injection of 1% pentobarbital at 50 mg/kg dosage, and then their limbs were fixed on the mouse board in a supine position. Use 18G intravenous indwelling for direct-view tracheal intubation for mice, and connect the small animal ventilator to adjust the parameters to assist ventilation. Open the chest layer by layer in the third 3/4 of the left margin of the mouse's chest. The left anterior descending coronary artery was ligated with a 7–0 round needle nylon suture. Close the chest layer by layer, suture the skin surgical incision, place the mouse on a constant temperature heating pad for recovery, closely observe the mouse's respiratory rate and nerve reflexes. After the mice return to spontaneous breathing and wake up, they were returned to the cage.

Mouse Heart Ultrasonography

One day before the operation of myocardial infarction model and 7 days and 28 days after myocardial infarction, the mice were used Vevo2000 small animal ultrasound system to perform transthoracic echocardiography to evaluate the cardiac function. After the mouse's chest area is depilated, the mouse is fixed in the supine position with tape on a 37°C constant temperature board, and the mouse's respiratory curve and electrocardiogram are recorded. Find the standard left ventricular long-axis view at the position of the left ventricular outflow tract, and then find the short-axis view perpendicular to the long axis, and collect an M-mode echocardiogram at the position of the middle section of the papillary muscle. Use M-mode echocardiography to measure at least 5 consecutive cardiac cycles, and calculate the left ventricular ejection fraction (LVEF) and the left ventricular short axis shortening rate (Left ventricular fractional shortening, LVFS).

Paraffin Section of Mouse Heart

The mice were anesthetized with an overdose of anesthetics, the chest and abdomen were cut open layer by layer, the heart and liver were exposed, and a cut was made at the liver. Firstly, 3% potassium chloride was injected from the apex to stop the heart, and then the heart apex was injected with pre-cooling immediately Wash the heart repeatedly with PBS buffer until the liver turns white. The heart was taken out, washed again in PBS buffer, and blotted dry with absorbent paper. The heart was immediately placed in a 10% neutral formaldehyde solution, fixed for 24–48 hours, dehydrated with gradient ethanol, and embedded in paraffin. Use a 4μm paraffin microtome to slice, bake the slices in a 60°C incubator for 1–2 hours, and store at room temperature.

Masson Staining

The Masson staining of heart section was detected via a Masson staining kit according to the manufacturer's instructions (Solarbio, Beijing, China). Routinely deparaffinize sections to water; Stain with the prepared Weigert iron hematoxylin staining solution for 5–10min; Differentiate with acidic ethanol for 5–15s, then wash with water; Masson blue liquid turns blue for 3–5min, then wash with water; Wash in distilled water for 1 min; Staining with Ponceau red fuchsin staining solution for 5–10min; In the above operation process, configure the weak acid working solution according to the ratio of distilled water: weak acid solution = 2:1, and wash with the weak acid working solution for 1 min; Wash with phosphomolybdic acid solution for 1–2min; Wash with a well-configured weak acid working solution for 1 min; Dye

directly in the aniline blue staining solution for 1–2min; Wash with a well-configured weak acid working solution for 1 min; quickly dehydrated in 95% ethanol; Dehydrate with absolute ethanol 3 times, 5–10s each time; Seal it with a neutral balsam containing xylene.

Isolation and Culture of Neonatal Rat Cardiomyocytes

The neonatal mice used in the experiment were all C57BL/6L newborn mice within 24 hours after birth. Sterilize the mice by immersing them in 75% alcohol for 30 seconds; Cut a small opening on the left side of the sternum from the midline of the left costal margin of the mouse with autoclaved ophthalmological scissors to squeeze out the heart; Cut the heart, then put the heart into the pre-cooled PBS buffer; After rinsing 3 sides with PBS buffer, cut the heart into 1mm3 tissue fragments with scissors; Transfer the tissue fragments into a 50mL centrifuge tube containing 10mL of 0.05% w/v trypsin/EDTA and 0.05% w/v collagenase for digestion, and digest for 10 minutes on a constant temperature shaker at 37 degrees Celsius; Centrifuge at low speed to get the precipitate, carefully pipet the supernatant and add it to the neutralizing medium (80% high-sugar DMEM and 20% fetal bovine serum) to stop the digestion; The precipitate obtained by centrifugation is digested by adding 10mL digestive enzyme, repeating the digestion 5–6 times, 10 minutes each time, until the tissue mass is basically digested; Pass all the digested products obtained through a 70mm sterile filter to remove undigested tissue fragments. Centrifuge at 1000 rpm again for 10 minutes, and the resulting pellet is myocardial cells; Resuspend the cell plate with an appropriate amount of high-sugar DMEM, and the fibroblasts that adhere to the wall first; After 1.5 hours, the non-adherent cells were aspirated, and then plated on a cell plate coated with 0.5% gelatin at a density of 1250 cells/mm2. DMEM cultured with neonatal rat cardiomyocytes contains 10% fetal bovine serum (FBS), 4.5 g/L glucose and 0.1 mM 5-bromo-2-deoxyuridine (BrdU); Cultivate the cardiomyocytes for 24–48 hours, do not move during this period, and perform follow-up experiments after the cells have fully adhered to the wall.

Cellular Immunofluorescence Staining

Fix the cell slide with 4% paraformaldehyde for 10 minutes, then rinse with PBS 3 times; Break the membrane with 0.1% Triton for 10 minutes, rinse 3 times with PBS and block with 3% BSA for 1 hour at room temperature. Incubate the primary antibody at 4°C overnight according to the recommended concentration of the antibody instruction. On the second day, rinse with PBS three times, then incubate the corresponding secondary antibody at room temperature for 1–2 hours, and rinse with PBS three times. Mount the slide with a mounting tablet containing DAPI.

Statistical Analysis

Statistical comparisons were performed using one- or two-way ANOVA and Student's *t* test for unpaired samples in ROS and apoptosis experiments. Prism 7.0 software (GraphPad Software) was used to assess the normality of the data and for statistical calculation. A p value of <0.05 was considered significant.

Results

Preparation of ROS-Responsive Nanoparticles Encapsulating Peptide

A schematic diagram of PEG-PPS-PEG polymer is shown in Figure 1A, which self-assembled into a vesicle structure with a diameter of about 50–180 nm(Figure 1B). In the presence of GHRH agonist MR409, the hydrophilic peptide was introduced into the inner space of the vesicle during the self-assembly process, which was named PEG-PPS-PEG @MR409 NPs. After H_2O_2 treatment for 48h, PPS were oxidized to convert the hydrophobic thioether to sulfoxide and finally hydrophilic sulfone, at which the particles were all disassembled and peptides were released. The average diameter of spherical vesicles was about 150±30 nm, which was independent of the polymer concentration (Figure 1C). Release of MR409 from the vesicles was effectively induced by H_2O_2, and reached to 90% after 72 h incubation, while only 30% MR409 was released with control water (Figure 1D).

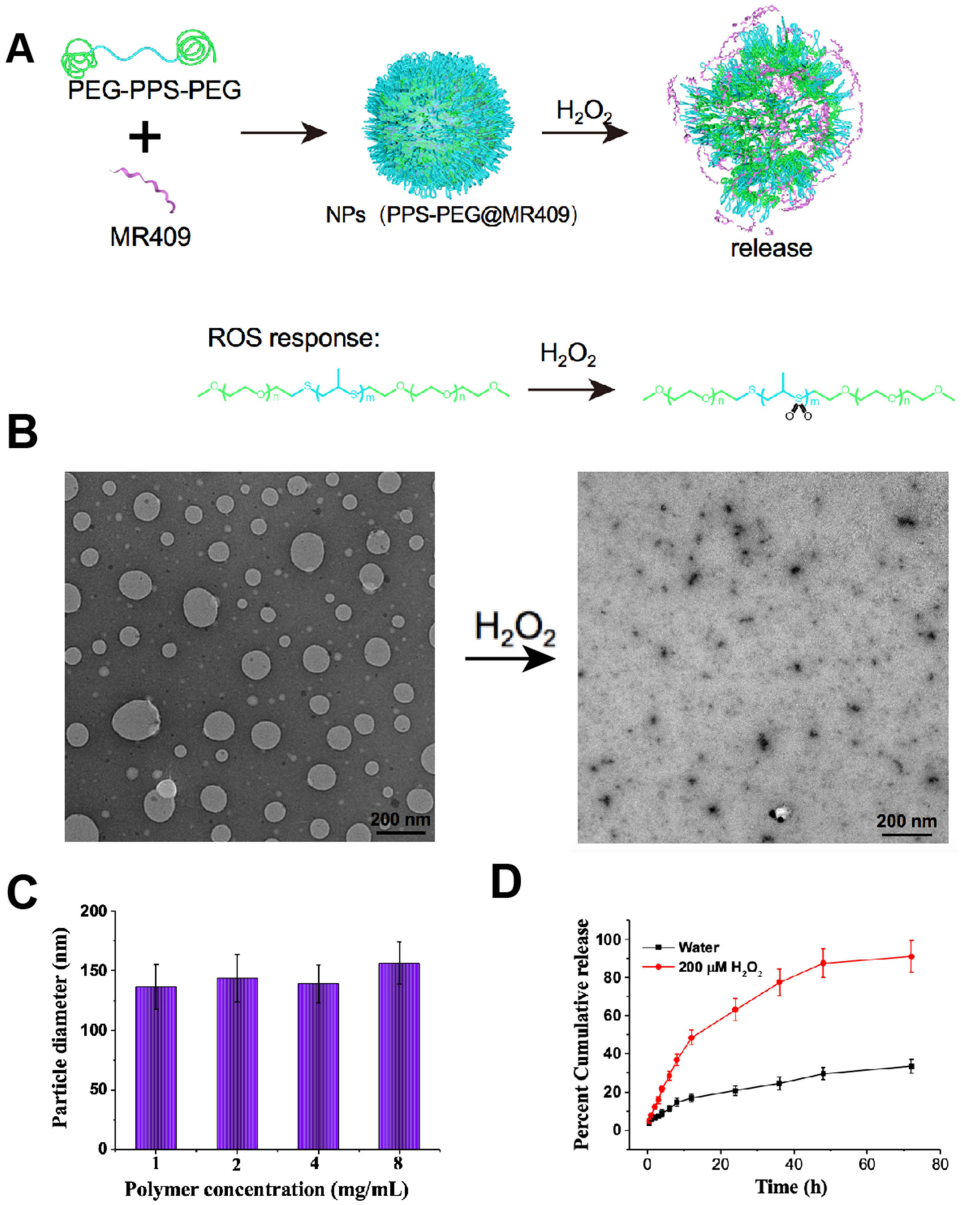

Figure 1 Synthesis and characterization of ROS-responsive vesicles encapsulating MR409. (**A**) Schematic diagram of ROS-responsive PEG-PPS-PEG vesicles with controlled release of peptide MR409; (**B**) Morphological change of PEG-PPS-PEG vesicles before and after H_2O_2 (200μmol) treatment; (**C**) PEG-PPS-PEG vesicle diameter; (**D**) In the presence of 200 μmol H_2O_2, MR409 was released cumulatively from PEG-PPS-PEG vesicles.

In vitro Cellular Uptake of PEG-PPS-PEG@MR409 NPs

Endocytosis of nanoparticles (NPs) is the first step toward intracellular delivery of the loaded drug molecules. We examined cellular uptake profiles in H9C2 rat ventricular cardiomyocytes (CMs), using FITC-labeled PEG-PPS-PEG@MR409 NPs (FITC/NP). After mixed FITC/NP with CM for 6 hours, a fluorescence signal around the nucleus was detected in a concentration-dependent manner (Figure 2A), indicating that the cells phagocytosed the NPs. FITC/NP can overlap with the cytoskeleton protein F-Actin (Figure 2B), confirming that the NPs were indeed phagocytosed by the cells.

In vitro Biological Activities of PEG-PPS-PEG@MR409 NPs

To determine whether PEG-PPS-PEG@MR409 NPs can reduce the deteriorative effects of ROS on cells, H9C2 cells and primary neonatal rat cardiomyocytes (NRCM) were cultured under normal condition or hypoxia and serum-free condition to simulate the environment of myocardial cells after myocardial infarction (MI). The production of ROS

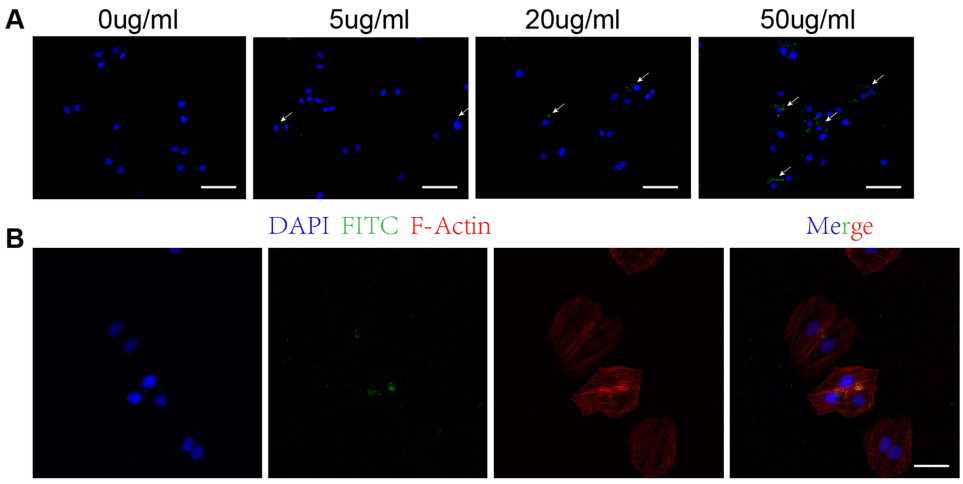

Figure 2 PEG-PPS-PEG@MR409 NPs were internalized by cardiomyocytes. (**A**) Fluorescence microscopic images (10X Objective) of H9C2 CMs after exposed to different concentrations of FITC-labeled PEG-PPS-PEG@MR409 NPs for 6 hours. Perinuclear aggregation of NPs was detected. The concentration refers to peptide. Bar:100uM. (**B**) Fluorescence microscopic images (20X Objective) of H9C2 CMs after mixed with 20 ug/mL FITC-labeled PEG-PPS-PEG@MR409 NPs for 6 hours. FITC/NP (green) was co-localized with F-Actin (red). Bar: 50uM.

from the CMs was reduced when MR409 or PEG-PPS-PEG or PEG-PPS-PEG@MR409 NPs was added to the culture (Figure 3A). The cell apoptosis induced by the hypoxia and serum-free culture condition was significantly reduced by the presence of PEG-PPS-PEG, MR409 and NPs (Figure 3B and C).

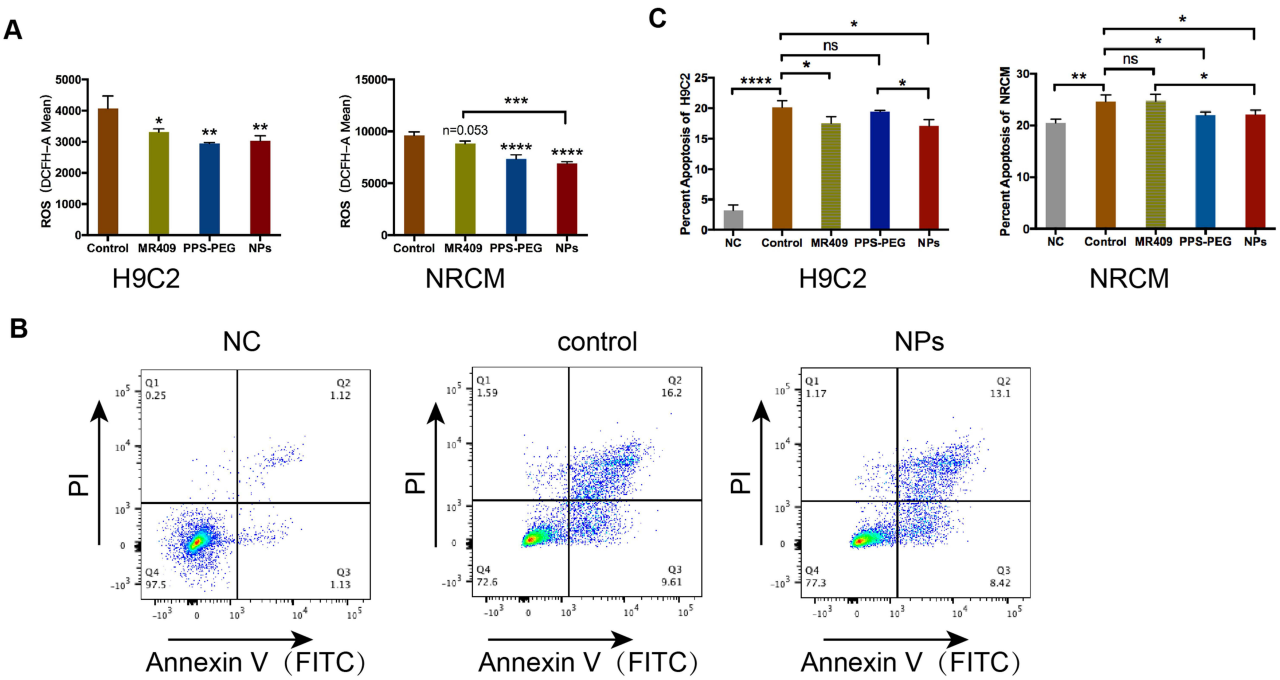

Figure 3 The effect of PEG-PPS-PEG@MR409 NPs on ROS production and apoptosis in CMs. Cells were cultured under normal condition, or hypoxia and serum-free condition for 24 hours, with or without PEG-PPS-PEG@MR409 NPs, or empty NP, or naked MR409 added to the culture. (**A**) The ROS produced by CMs were analyzed by fluorescent staining with DCFH-A and quantified by flow cytometry; (**B**) Representative pictures show flow cytometry assay of H9C2 cells after staining with Annexin V (FITC) and PI. (**C**). The positive ratio of Annexin IV and PI positive cells was quantified, representing the level of apoptosis.
Notes: * P<0.05, ** P<0.01, *** P<0.001, **** P<0.0001, ns: no statistical difference.

In vivo Targeting Ability of PEG-PPS-PEG@MR409 NPs to the Infarcted Heart

To investigate the targeting ability of the PEG-PPS-PEG@MR409 to the infarcted heart, MR409 peptide was labelled with the fluorescent probe Cy5 (PEG-PPS-PEG@MR409-Cy5). The PEG-PPS-PEG@MR409-Cy5 were subcutaneously injected into mice after MI procedure. The biodistribution of PEG-PPS-PEG@MR409-Cy5 in mice post-MI was analyzed by fluorescent imaging at different time points post-injection (Figure 4A). Liver and kidney had the highest fluorescence intensity in both MI and non-MI mice at all time points. The relative fluorescence intensity was significantly higher in the infarcted hearts than that in the normal hearts (Figure 4B), indicating that the PEG-PPS-PEG@MR409 NPs NPs can actively aggregate onto the infarcted heart.

Targetable Delivery of PEG-PPS-PEG@MR409 NPs to Infarct Heart

To further confirm the PEG-PPS-PEG@MR409 NPs are ROS responsive and can aggregate onto the infarcted heart, we injected MR409-Cy5 with or without PEG-PPS-PEG material into mice 10 minutes after myocardial infarction. The fluorescence signal in the heart from PEG-PPS-PEG@MR409 injected mice was significantly higher (~10%) than that with naked MR409-Cy5 (Figure 5A and B). Furthermore, a strong fluorescence signal could be detected in the ligation position of the heart (Figure 5C). These results show that PEG-PPS-PEG@MR409 could efficiently deliver MR409 peptide to the injured site.

ROS-Responsive PEG-PPS-PEG@MR409 NPs Improved Cardiac Functions of the Infarct Heart

To evaluate the therapeutic effect of the ROS-responsive PEG-PPS-PEG@MR409 NPs on myocardial infarction, the NPs or naked MR409 was injected via the tail vein once every three days or once a day, respectively, for 14 consecutive days (detail in Materials and Methods). The dose of MR409 group was 5ug/mouse/day, PEG-PPS-PEG@MR409 NPs group received 15ug/mouse/3 day (Figure 6A). Cardiac systolic functions significantly increased after treatment with either MR409 or PEG-PPS-PEG@MR409 NPs at 28 days after MI, compared to PBS or PEG-PPS-PEG treatment (Figure 6B). The infarct size was also significantly reduced in the MR409 or PEG-PEG-PPS-PEG@MR409 NPs treated mice (Figure 6C and D). There was no significant difference in heart function between MR409 and PEG-PPS-PEG @MR409 NPs groups (Figure 6B-D). Considering that one-third of the injection frequency was used for NPs compared to MR409, these results indicate that PEG-PPS-PEG@MR409 NPs can reduce the number of administrations while exerting a similar therapeutic effect as naked MR409.

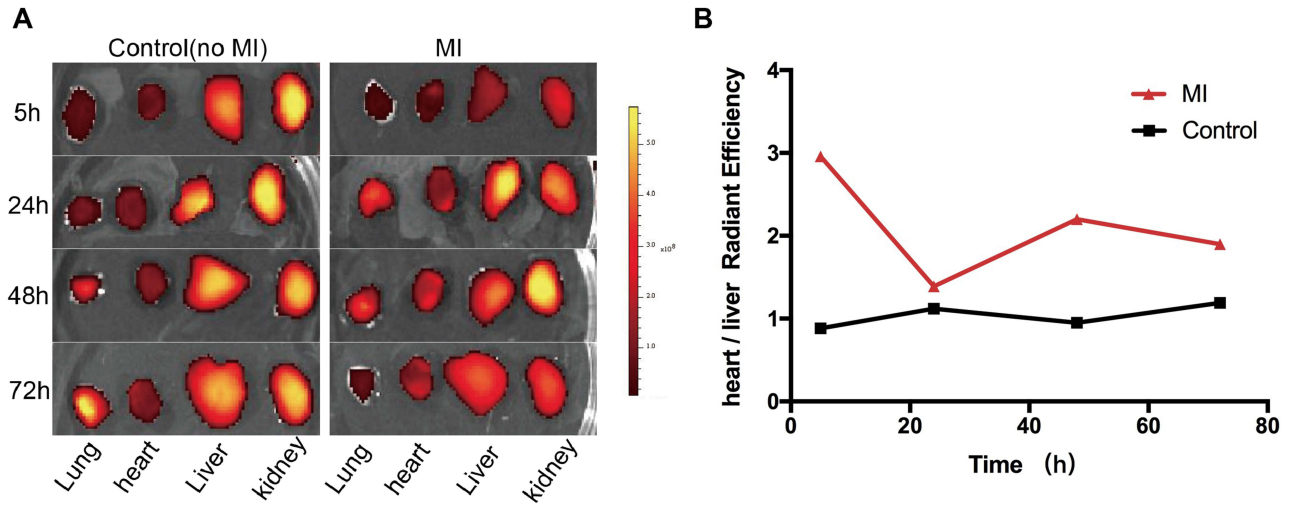

Figure 4 Aggregation of PEG-PPS-PEG@MR409 NPs onto the different tissues. Cy5-labeled nanoparticles were subcutaneously injected into mice at 10 min after myocardial infarction. (**A**) The aggregation of nanoparticles in the lung, heart, liver, and kidney was observed at 5h, 24h, 48h, and 72h; (**B**) Quantification of the fluorescence intensity in hearts, which was expressed in a ratio of heart to liver.

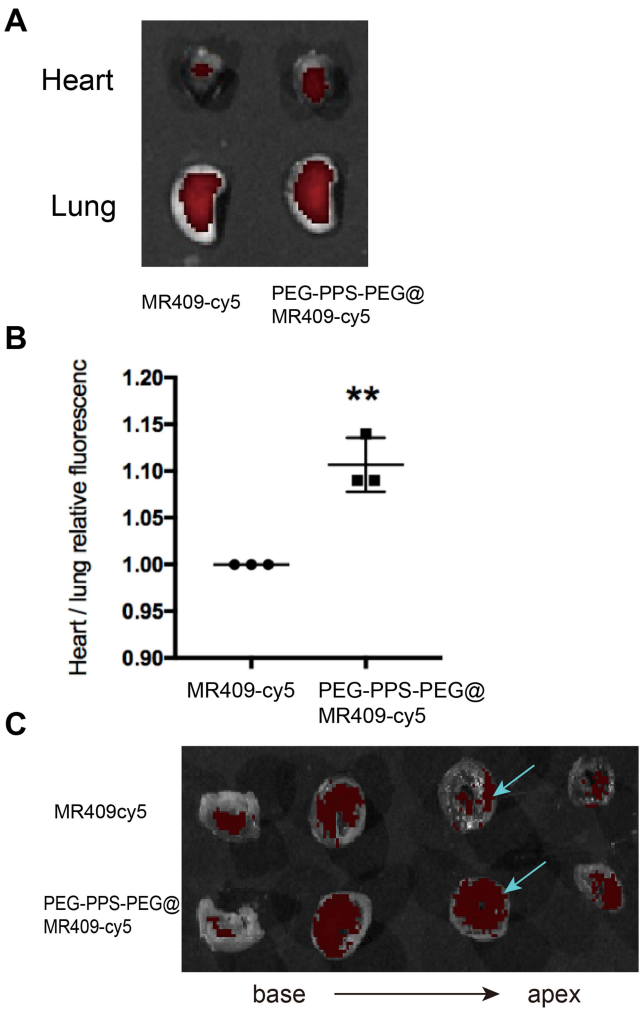

Figure 5 Targeting delivery of MR409 peptide by PEG-PPS-PEG vesicles onto the infarct heart. MR409-Cy5 or PEG-PPS-PEG@MR409-Cy5 NPs were IV injected into mice 10 min post MI procedure. Hearts and lungs were collected 30 min later. (**A**) Fluorescence images of the heart and lungs; (**B**) Quantification of fluorescence intensity ratio of heart to lung; (**C**) The fluorescence images of four equal parts of a heart that was cut vertically from the base to the apex; Blue arrow points the ligation position. More red fluorescence was observed at the ligation site.
Note: ** p<0.01, n=3.

Discussion

In this research, we presented an innovative method for cardiac delivery of peptide drugs using a ROS-sensitive nanoparticle (NP) system. The NPs not only can deliver peptide drugs to the heart but also directly reduced the ROS level at the injured site, resulted in more efficient therapeutic effect for the infarcted heart as compared to the use of naked peptides. The NPs released the peptide drug in an ROS-responsive manner and were targeted to the infarct heart, which significantly reduced CM apoptosis and cardiac fibrosis.

Effective delivery of peptide drugs to the heart has long been a challenge. Typically, peptide drugs are administered via subcutaneous injection, which is inconvenient. Although hormone peptide drugs have the advantages of high sensitivity and specificity, they are difficult to deliver effectively and require high doses, leading to side effects.[20] By applying a ROS-responsive nanocoat to the peptide, we not only protect the peptide but also target it to the injured heart for more efficient, faster, and effective therapy. The main advantages of this drug delivery system are: 1) Passive targeting by ROS response increases the drug concentration at the lesion site while reducing its distribution in non-targeted tissues and organs, thus minimizing adverse drug reactions; 2) The number of drug injections needed is reduced to achieve similar therapeutic effects compared to naked peptide administration.

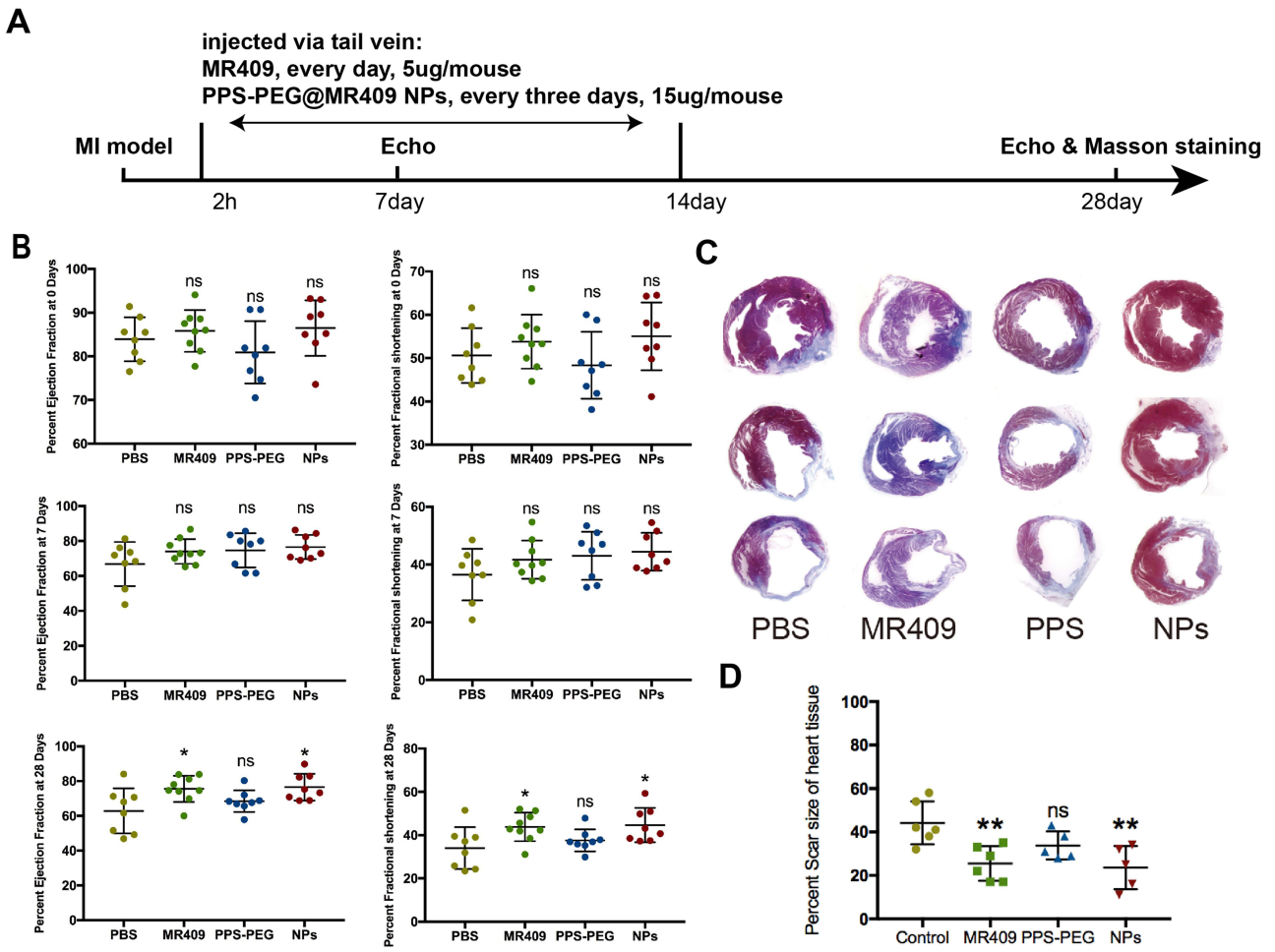

Figure 6 PEG-PPS-PEG@MR409 NPs improved cardiac functions of infarct heart. (**A**) Schematic time line of mice experiment. After MI procedure, PBS (NC) or naked MR409 peptide (MR409), or empty PEG-PPS-PEG was injected via the tail vein once a day for 14 consecutive days; PEG-PPS-PEG@MR409 NPs (NPs) was injected similarly once every 3 days for 14 consecutive days. (**B**) The ejection fraction (EF) and fractional shortening (FS) of the mouse heart were detected by ultrasound at 0, 7, and 28 days after injection; (**C**) Masson & Trichrome stained sections of a heart that were recovered at 28 days post MI. (**D**) Quantification of the scar size.
Notes: ** P<0.01, n=5-6.

Nanodrug delivery system has a strong vascular penetration ability, particularly for newly formed vasculature and ischemia-damaged vessels.[22–26] Due to the abundant blood vessels, large vascular space, and the lack of lymphatic drainage in tumor tissues, the nano drug-carrying system can form a drug-rich microenvironment around the tumor tissue. Therefore, nano drug delivery systems are widely used in solid tumors.[27,28] Following MI injury, vascular endothelial impairment and new capillaries are common around the ischemic area, creating a permeable local micro-environment for nanodrug delivery.[29] Our results demonstrated that PEG-PPS-PEG@MR409 NPs aggregated onto the infarcted heart (Figure 5). Besides targeted delivery, PEG-PPS-PEG@MR409 NPs may consume some ROS, thereby reducing ischemic damage to the CMs. Our data showed that PEG-PPS-PEG can reduce CM apoptosis caused by ROS (Figure 3). Combining these benefits, we demonstrated that the PEG-PPS-PEG -encapsulated peptide is superior to naked peptide for therapeutic effect. Without altering the total amount of the MR409 peptide, PEG-PPS-PEG@MR409 NPs required only one-third the number of injections to achieve the same therapeutic effect on myocardial infarction as the naked MR 409 (Figure 6).

Studies have shown that the nanodrug delivery system can be recognized and phagocytosed by mononuclear-phagocytic immune cells in blood, liver, spleen, and lymphatic system. After uptake, immune cells migrated to the inflammatory sites to realize a new nano-drug delivery mechanism.[30] Our data showed that CMs could uptake the PEG-

PPS-PEG@MR409 NPs (Figure 2). Further investigation is needed to determine whether immune cells deliver PEG-PPS -PEG@MR409 NPs to the infarct heart.

Although the PEG-PPS-PEG@MR409 NPs achieved targeted release, and reduced the number of injections, this design has certain limitations: 1) Compared to the peptide without PEG-PPS-PEG coating, targeting efficiency has been increased by only 10% 30 minutes after myocardial infarction (Figure 5C), indicating room for improvement; 2) While nanoparticles between 20–200 nm can remain in circulation longer, the majority are metabolized by the liver and kidney, with only a few reaching the heart;[31] 3) The safety of nanocarriers and their in vivo fate still require thorough investigation. Therefore, further research is necessary to fully understand the targeted release of peptide drugs in vivo.

Conclusion

We demonstrated that PEG-PPS-PEG@MR409 NPs can effectively target the myocardial injury site to deliver MR409 peptide. Additionally, the material itself can reduce ROS levels and prevent CM apoptosis. PEG-PPS-PEG@MR409 NPs achieved more efficient therapeutic effects on myocardial infarction compared to MR409 alone. Although the exact mechanism needs further investigation, this research proposes a novel method for targeted treatment of myocardial infarction using peptide drugs and presents a new approach for heart disease therapy.

Acknowledgments

This research work was supported by grants from the National Natural Science Foundation of China (No. 82070448 to HY) (No. 82202357 to XPP) (No. 82200434 to LQ), Self research project of Zhejiang University Binjiang Research Institute (No. ZY202205SMKY008 to HY) and the Medicine and Health Science and Technology Project of Zhejiang Province (No. 2024KY1071 to YPW). We thank Dr. Zhengwei Mao for providing the materials and assistance for the experiments.

Disclosure

The authors declare no competing interest in this work.

References

1. Feng J, Zhang Y, Zhang J. Epidemiology and burden of heart failure in Asia. *JACC Asia*. 2024;4(4):249–264. doi:10.1016/j.jacasi.2024.01.013
2. Granata R, Trovato L, Gallo MP, et al. Growth hormone-releasing hormone promotes survival of cardiac myocytes in vitro and protects against ischaemia-reperfusion injury in rat heart. *Cardiovasc Res*. 2009;83(2):303–312. doi:10.1093/cvr/cvp090
3. Kanashiro-Takeuchi RM, Tziomalos K, Takeuchi LM, et al. Cardioprotective effects of growth hormone-releasing hormone agonist after myocardial infarction. *Proc Natl Acad Sci*. 2010;107(6):2604–2609. doi:10.1073/pnas.0914138107
4. Penna C, Settanni F, Tullio F, et al. GH-releasing hormone induces cardioprotection in isolated male rat heart via activation of RISK and SAFE pathways. *Endocrinology*. 2013;154(4):1624–1635. doi:10.1210/en.2012-2064
5. Kanashiro-Takeuchi RM, Takeuchi LM, Rick FG, et al. Activation of growth hormone releasing hormone (GHRH) receptor stimulates cardiac reverse remodeling after myocardial infarction (MI). *Proc Natl Acad Sci*. 2012;109(2):559–563. doi:10.1073/pnas.1119203109
6. Izdebski J, Pinski J, Horvath JE, et al. Synthesis and biological evaluation of superactive agonists of growth hormone-releasing hormone. *Proc Natl Acad Sci*. 1995;92(11):4872–4876. doi:10.1073/pnas.92.11.4872
7. Ludwig B, Ziegler CG, Schally AV, et al. Agonist of growth hormone-releasing hormone as a potential effector for survival and proliferation of pancreatic islets. *Proc Natl Acad Sci*. 2010;107(28):12623–12628. doi:10.1073/pnas.1005098107
8. Granata R. Peripheral activities of growth hormone-releasing hormone. *J Endocrinol Invest*. 2016;39(7):721–727. doi:10.1007/s40618-016-0440-x
9. Shen J, Zhang N, Lin YN, et al. Regulation of vascular calcification by growth hormone-releasing hormone and its agonists. *Circ Res*. 2018;122 (10):1395–1408. doi:10.1161/CIRCRESAHA.117.312418
10. Giardiello M, Liptrott NJ, McDonald TO, et al. Accelerated oral nanomedicine discovery from miniaturized screening to clinical production exemplified by paediatric HIV nanotherapies. *Nat Commun*. 2016;7(1):13184. doi:10.1038/ncomms13184
11. Kim BY, Rutka JT, Chan WC. Nanomedicine. *N Engl J Med*. 2010;363(25):2434–2443. doi:10.1056/NEJMra0912273
12. Davis ME, Zuckerman JE, Choi CH, et al. Evidence of RNAi in humans from systemically administered siRNA via targeted nanoparticles. *Nature*. 2010;464(7291):1067–1070. doi:10.1038/nature08956
13. Weissig V, Pettinger TK, Murdock N. Nanopharmaceuticals (part 1): products on the market. *Int J Nanomed*. 2014;9:4357–4373. doi:10.2147/IJN.S46900
14. Kuai R, Ochyl LJ, Bahjat KS, et al. Designer vaccine nanodiscs for personalized cancer immunotherapy. *Nat Mater*. 2017;16(4):489–496. doi:10.1038/nmat4822
15. Zhao Y, Fay F, Hak S, et al. Augmenting drug-carrier compatibility improves tumour nanotherapy efficacy. *Nat Commun*. 2016;7(1):11221. doi:10.1038/ncomms11221

16. Tiwari G, Tiwari R, Sriwastawa B, et al. Drug delivery systems: an updated review. *Int J Pharm Investig*. 2012;2(1):2–11. doi:10.4103/2230-973X.96920
17. Lee SH, Gupta MK, Bang JB, et al. Current progress in Reactive Oxygen Species (ROS)-responsive materials for biomedical applications. *Adv Healthc Mater*. 2013;2(6):908–915. doi:10.1002/adhm.201200423
18. Xu Q, He C, Xiao C, et al. Reactive Oxygen Species (ROS) responsive polymers for biomedical applications. *Macromol Biosci*. 2016;16 (5):635–646. doi:10.1002/mabi.201500440
19. Ziegler M, Xu XQ, Yap ML, et al. A self-assembled fluorescent nanoprobe for imaging and therapy of cardiac ischemia/reperfusion injury. *Adv Ther*. 2019;2(3):1800133. doi:10.1002/adtp.201800133
20. Miragoli M, Ceriotti P, Iafisco M, et al. Inhalation of peptide-loaded nanoparticles improves heart failure. *Sci Transl Med*. 2018:10. 10.1126/scitranslmed.aan6205
21. Zhao Y, Zhu J, Zhang N, et al. GDF11 enhances therapeutic efficacy of mesenchymal stem cells for myocardial infarction via YME1L-mediated OPA1 processing. *Stem Cells Transl Med*. 2020;9(10):1257–1271. doi:10.1002/sctm.20-0005
22. Acharya S, Sahoo SK. PLGA nanoparticles containing various anticancer agents and tumour delivery by EPR effect. *Adv Drug Deliv Rev*. 2011;63 (3):170–183. doi:10.1016/j.addr.2010.10.008
23. Baxter GF. The neutrophil as a mediator of myocardial ischemia-reperfusion injury: time to move on. *Basic Res Cardiol*. 2002;97(4):268–275. doi:10.1007/s00395-002-0366-7
24. Li Y, Xu P, He D, et al. Long-circulating thermosensitive liposomes for the targeted drug delivery of oxaliplatin. *Int J Nanomed*. 2020;15:6721–6734. doi:10.2147/IJN.S250773
25. Markman JL, Rekechenetskiy A, Holler E, et al. Nanomedicine therapeutic approaches to overcome cancer drug resistance. *Adv Drug Deliv Rev*. 2013;65(13–14):1866–1879. doi:10.1016/j.addr.2013.09.019
26. Takahama H, Minamino T, Asanuma H, et al. Prolonged targeting of ischemic/reperfused myocardium by liposomal adenosine augments cardioprotection in rats. *J Am Coll Cardiol*. 2009;53(8):709–717. doi:10.1016/j.jacc.2008.11.014
27. Nishiyama N, Okazaki S, Cabral H, et al. Novel cisplatin-incorporated polymeric micelles can eradicate solid tumors in mice. *Cancer Res*. 2003;63 (24):8977–8983.
28. Mochida Y, Cabral H, Miura Y, et al. Bundled assembly of helical nanostructures in polymeric micelles loaded with platinum drugs enhancing therapeutic efficiency against pancreatic tumor. *ACS Nano*. 2014;8(7):6724–6738. doi:10.1021/nn500498t
29. van Bochove GS, Paulis LE, Segers D, et al. Contrast enhancement by differently sized paramagnetic MRI contrast agents in mice with two phenotypes of atherosclerotic plaque. *Contrast Media Mol Imaging*. 2011;6(1):35–45. doi:10.1002/cmmi.402
30. Flogel U, Ding Z, Hardung H, et al. In vivo monitoring of inflammation after cardiac and cerebral ischemia by fluorine magnetic resonance imaging. *Circulation*. 2008;118(2):140–148. doi:10.1161/CIRCULATIONAHA.107.737890
31. Petros RA, DeSimone JM. Strategies in the design of nanoparticles for therapeutic applications. *Nat Rev Drug Discov*. 2010;9(8):615–627. doi:10.1038/nrd2591